

N87-22227

INFLUENCE OF TORSIONAL-LATERAL COUPLING ON STABILITY

BEHAVIOR OF GEARED ROTOR SYSTEMS*

P. Schwibinger and R. Nordmann
University of Kaiserslautern
Kaiserslautern, Federal Republic of Germany

In high-performance turbomachinery trouble often arises because of unstable nonsynchronous lateral vibrations. The instabilities are mostly caused by oil-film bearings, clearance excitation, internal damping, annular pressure seals in pumps, or labyrinth seals in turbocompressors. In recent times the coupling between torsional and lateral vibrations has been considered as an additional influence. This coupling is of practical importance in geared rotor systems. The literature (refs. 1 and 2) describes some field problems in geared drive trains where unstable lateral vibrations occurred together with torsional oscillations. This paper studies the influence of the torsional-lateral coupling on the stability behavior of a simple geared system supported by oil-film bearings. The coupling effect is investigated by parameter studies and a sensitivity analysis for the uncoupled and coupled systems.

INTRODUCTION

The dynamic behavior of many rotating machines (e.g., turbines and compressor pumps) is influenced by the stiffness and damping characteristics of nonconservative effects such as oil-film forces, forces in seals, and clearing excitation forces. Besides the forced unbalance vibrations, unstable nonsynchronous vibrations caused by such self-exciting mechanisms may also occur. Usually the stability analysis for this turbomachinery is limited to a lateral rotor dynamic analysis that is carried out independently from the torsional vibration analysis. However, for geared rotor systems - that is, compressor or turbogenerator sets (fig. 1) - the torsional and lateral vibrations are coupled because of the offset centerlines of the geared rotors. Previously we did not know how much this coupling affected the stability of the machine.

In the literature we find several publications concerning torsional-lateral coupling in high-performance turbomachinery with gears. Wachel and Szenasi (ref. 1) describe a field problem in a geared system where unstable lateral vibrations occurred together with torsional oscillations. The authors do not describe the coupling mechanisms, but they point out the importance of gears for the exchange of energy between torsional and lateral vibrations. Similar instability phenomena were observed on different units. Yamada and Mitsui (ref. 2) deal with a two-stage ship gear supported by oil-film bearings. During operation with partial load the pinion ran unstably. A coupled torsional-lateral analysis limited to the gear stage shows that the oil-film

*This research work was supported by Deutsche Forschungsgemeinschaft, German Federal Republic.

bearings are the source of instability, but the stability threshold is decisively influenced by the torsional stiffness of the rotor system. Iannuzzelli and Elward (ref. 3) point out that certain measured eigenfrequencies of a compressor train can be verified only by an analytical model that considers the torsional-lateral coupling in a gear stage. Simmons and Smalley (ref. 4) found by experimental and analytical investigations of a gas turbine/compressor train that torsional modes (i.e., coupled torsional-lateral modes) with a superposed bending component at the gear wheel can be damped significantly by the oil-film bearings.

This paper investigates the influence of the torsional-lateral coupling in the gear on the stability behavior of a simple geared system (fig. 2). The coupling effect is analyzed by means of parameter studies and a sensitivity analysis for the uncoupled and coupled systems.

NATURAL VIBRATIONS OF GEARED ROTOR SYSTEM

Mechanical Model

Figure 1 shows a typical turbomachine consisting of two elastic shafts connected by a reduction gear. The rotors run in oil-film bearings. Usually the lateral vibration analysis (including a stability analysis) is carried out for both shafts separately and independently from the torsional rotor dynamics analysis. But in fact torsional and lateral vibrations of both rotors are coupled by the gear. To study whether this coupling may really be ignored in a stability analysis, we first consider a simple geared rotor system. Figures 2 and 3 show the model with two elastic shafts connected by a gear. The axes of the shafts are offset by the angle of mesh so that the tooth force acts in the vertical plane on the gear wheels. Both shafts are elastic for torsion and bending. Shaft 1 runs in two identical oil-film bearings that are the only source of instability in the system. Shaft 2 is supported rigidly. Note that not all the effects of the real machine can be investigated with the simple model. We concentrate on the coupling effect in the gear stage and its interaction with the self-excited vibrations of the vibration system.

In a gear a strong torsional-lateral coupling exists naturally because of the mechanism of power transmission. The torsional moment fed into the gear is transmitted by tooth forces. For that reason transverse forces and bending moments result from the torsional moment. Also the torsional and lateral displacements of the gear wheels are coupled kinematically (fig. 4), provided that both wheels maintain contact during operation. Without the lateral displacement of the gear wheels the kinematic relation in a gear stage is

$$r_1 q_1 = r_2 q_2 \quad (1)$$

This is the model commonly used in rotor dynamics analysis. If we allow lateral movement of the gear wheels, the geometric equation

$$r_1 q_1 + q_3 = r_2 q_2 + q_4 \quad (2)$$

implies a coupling of the torsional and lateral degrees of freedom.

From the theoretical considerations it is known that, for small vibrations of the journal bearings around a static equilibrium position, there is a linear force motion relation for the oil film (fig. 5):

$$\begin{bmatrix} \Delta f_1 \\ \Delta f_2 \end{bmatrix} = - \begin{bmatrix} c_{11} & c_{12} \\ c_{21} & c_{22} \end{bmatrix} \cdot \begin{bmatrix} \dot{q}_1 \\ \dot{q}_2 \end{bmatrix} - \begin{bmatrix} k_{11} & k_{12} \\ k_{21} & k_{22} \end{bmatrix} \begin{bmatrix} q_1 \\ q_2 \end{bmatrix} \quad (3)$$

where

k_{ik} stiffness coefficients of bearings

c_{ik} damping coefficients of bearings

The stiffness and damping coefficients depend on the rotational speed and the static load on the bearing. The resulting static equilibrium position of the shaft in the journal bearing is characterized by the dimensionless Sommerfeld number. In addition, the bearing coefficients depend on the load direction, which must be taken into consideration for geared rotors, where the gear transmission forces often make up an appreciable part of the bearing load. Available data for these coefficients assume a specific load direction (gravity load direction), but in a geared rotor system the load direction may be different because it is governed by the gear mesh forces. Hence, if the bearing geometry is such that the coefficients are sensitive to load direction, they must be calculated by solving the lubrication equation or by using an approximate formula (refs. 5 and 6). As the coefficients normally are obtained in a bearing coordinate system that does not coincide with the chosen system for the geared rotor, a transformation must be performed. Besides being anisotropic, the stiffness cross-coupling terms are generally unequal. This asymmetry is the reason for self-excited shaft vibrations.

For the statically indeterminate supported shaft in journal bearings, the calculation of the static load in the bearings leads to a nonlinear problem that has to be solved numerically. The reason for this is the nonlinear force-motion relation in the journals. In our study the static bearing loads due to the transmitted power and rotor weight are estimated with the rigidly supported shaft system.

An energy-flow diagram demonstrates how self-excited bending vibrations in a geared system may exchange energy with torsional oscillations by means of the gear mechanism (fig. 6). The main energy flows from the motor to the generator to transmit the required power for the unit. Because of shear forces in the oil film of the journal bearing, energy branches off from the main flow to the bearing, where it may dissipate from oil-film friction or may excite bending vibrations in the shaft and the gear. Because torsional and bending displacements are coupled in the gear stage, torsional oscillations of the geared rotor train also are excited. It is clear from these considerations that the stability behavior is affected by this energy exchange between the torsional and the lateral system.

Equations of Motion

To obtain the equations of motion for the simple shaft system (fig. 2) with N degrees of freedom, we apply the principle of virtual work. Using static deflection functions for the approximation of the displacements, we can discretize the model with continuous mass and stiffness distribution into disk, shaft, and bearing elements connected at their nodes. The resulting energy equation expresses that the sum of the virtual work done by the inertia, damping, stiffness, and external forces is equal to zero:

$$\delta \underline{q}^T \{ \underline{M} \ddot{\underline{q}} + \underline{D} \dot{\underline{q}} + \underline{K} \underline{q} - \underline{f}(t) \} = 0 \quad (4)$$

where

\underline{M} ($N \times N$) mass matrix

\underline{D} ($N \times N$) damping matrix

\underline{K} ($N \times N$) stiffness matrix

\underline{q} ($N \times 1$) vector of displacements

\underline{f} ($N \times 1$) vector of external forces

To connect both shafts, we introduce the kinematic relation of equation (1) for the uncoupled system and of equation (2) for the torsional-lateral-coupled system by the matrix equation

$$\underline{q} = \underline{I} \cdot \tilde{\underline{q}} \quad (5)$$

where

$$\underline{q} = \begin{bmatrix} \cdot \\ \cdot \\ q_1 \\ q_2 \\ q_3 \\ q_4 \\ \cdot \\ \cdot \\ \cdot \end{bmatrix} \begin{matrix} 1 \\ \cdot \\ \cdot \\ \cdot \\ \cdot \\ \cdot \\ \cdot \\ \cdot \\ N \end{matrix} \quad \text{and} \quad \tilde{\underline{q}} = \begin{bmatrix} \cdot \\ \cdot \\ q_1 \\ q_3 \\ q_4 \\ \cdot \\ \cdot \\ \cdot \\ \cdot \end{bmatrix} \begin{matrix} 1 \\ \cdot \\ \cdot \\ \cdot \\ \cdot \\ \cdot \\ \cdot \\ \cdot \\ \tilde{N} \end{matrix}$$

Natural Vibrations - Eigenvalues and Natural Modes

The natural vibrations can be calculated from the homogeneous equations of motion ($\underline{\ddot{f}} = 0$).

Assuming a solution of the form $\underline{\tilde{q}}(t) = \underline{r} \cdot e^{\lambda t}$, we obtain the quadratic eigenvalue problem

$$(\lambda^2 \underline{\tilde{M}} + \lambda \underline{\tilde{D}} + \underline{\tilde{K}}) \underline{r} = \underline{0} \quad (7)$$

with $2N$ eigenvalues λ_j and corresponding eigenvectors \underline{r}_j . In most cases eigenvalues as well as eigenvectors occur in conjugate complex pairs:

$$\begin{aligned} \text{Eigenvalues} - \lambda_j &= \alpha_j + i\omega_j & \bar{\lambda}_j &= \alpha_j - i\omega_j \end{aligned} \quad (8)$$

$$\begin{aligned} \text{Eigenvectors} - \underline{r}_j &= \underline{s}_j + i\underline{t}_j & \bar{\underline{r}}_j &= \underline{s}_j - i\underline{t}_j \end{aligned}$$

We consider only the part of the solution that belongs to a conjugate complex pair:

$$\underline{\tilde{q}}_j(t) = B_j e^{\alpha_j t} \{ \underline{s}_j \sin(\omega_j t + \gamma_j) + \underline{t}_j \cos(\omega_j t + \gamma_j) \} \quad (9)$$

where ω_j is the circular natural frequency of this part and α_j the damping constant. If the damping constant $\alpha_j > 0$, the natural vibrations increase and make the system unstable, if $\alpha_j < 0$, the natural vibrations decrease and the system runs stably.

For the torsional-lateral-coupled system the eigenvalues are composed of torsional-lateral-coupled damping constants and eigenfrequencies. The corresponding modes are set up by torsional and lateral components. We define the expression in braces of equation (9) as the natural mode. In contrast to conservative systems there is no constant modal shape: proportions and relative phasing generally vary from point to point at the shaft. The lateral components of one natural mode represent a time-dependent curve in space. The plane of motion of one point of the shaft has an elliptical orbit. The torsional components of one natural mode also twist the shaft along its axis.

If we transpose the matrices $\underline{\tilde{M}}$, $\underline{\tilde{D}}$, and $\underline{\tilde{K}}$, we obtain the so-called left-hand eigenvalue problem

$$\{ \lambda^2 \underline{\tilde{M}}^T + \lambda \underline{\tilde{D}}^T + \underline{\tilde{K}}^T \} \underline{l} = \underline{0} \quad (10)$$

which has the same eigenvalues λ but different eigenvectors \underline{l} . Both eigenvector sets are needed to decouple the system matrices for the sensitivity analysis of the eigenvalues.

First the eigenfrequencies and modes for the rigidly supported system are calculated in the manner described. A similar system was studied by Iida (ref. 8). Because of its geometry (fig. 3), for bending purposes shaft 2 is very stiff as compared with shaft 1. Figure 7 shows the natural modes of vibration where the torsional displacement of shaft 1 is multiplied by the radius of gear wheel 1 and the twisting of shaft 2 is multiplied by the radius of gear wheel 2 to match the dimension with the bending. With this

normalization the kinematic constraint equation (1) equation (2) can be verified at once from the plot of the eigenvectors, because the sum of torsional and lateral displacement at shaft 1 and shaft 2 must be equal at the gear mesh.

In the first mode the torsional displacement is rather predominant, but in the second and fourth modes it is comparable to the flexural displacement. In these two modes the eigenfrequencies of the torsional-lateral-coupled system differ about 15 and 5 percent, respectively, from the solutions of the uncoupled system. The third eigenvector lies in the x-y plane, which is perpendicular to the direction of the tooth force. Therefore for the rigidly supported system it is a completely decoupled bending mode.

When the coupling effect has such a strong influence on the eigenfrequencies, how does it affect the damping constants of the eigenvalues for the oil-film-supported system in figure 2? To answer this question, we calculate the eigenvalues for the uncoupled and coupled systems. Because the bearing coefficients depend on both the rotational speed and the static load on the journal, the eigenvalues change with the running speed and the transmitted load.

In figure 8, for the six lowest eigenvalues, the eigenfrequencies ($f = \omega/2\pi$ rpm) and damping coefficients ($a = \alpha/2\pi$ rpm) are plotted as a function of the rotational speed of shaft 1 for the uncoupled system (---) and for the torsional-lateral-coupled system (_____). In this diagram the static load on the bearings remains constant during the alteration of shaft speed. Static load is determined by the weight of the shaft and the transmitted moment M_M or M_G (fig. 3).

It is obvious that most of the eigenfrequencies change only little and that they almost coincide with the solutions for the rigidly supported system. The reason for this is that the oil-film bearings in the investigated speed range are relatively stiff as compared with the elasticity of the shaft. Exceptions are the two whirling frequencies, which grow linearly with the rotor speed. Their frequency is approximately one-half the speed of shaft 1. They belong to highly damped modes where the movement of the oil-film-supported shaft represents a conical whirl in one of the two bearings.

In some modes the frequencies for the uncoupled and torsional-lateral-coupled systems differ essentially (e.g., the second frequency of the coupled system is about 15 percent lower than that for the uncoupled system). Figure 9 shows the strong torsional-lateral coupling in the corresponding eigenmode in contrast to the first eigenvector, which remains an almost pure torsional mode even in the coupled model.

The coupling affects not only the eigenfrequencies and modes but also the damping constants (fig. 8). The zero passage of one damping coefficient indicates the stability threshold of the system. In the uncoupled system all the damping constants for the bending modes are negative up to a threshold speed of 3745 rpm, where the first bending mode ($f_2 = 2157$ rpm) becomes unstable. It proves that the dangerous positive damping constants occur at the lower bending eigenvalues. Because we have not introduced additional torsional damping, the damping constants for the torsional modes ($f_1 = 821$ rpm, $f_4 = 4370$ rpm) are equal to zero.

In the torsional-lateral-coupled system the lateral motion of the shaft in the journals may contribute additional damping to the torsional modes (fig. 6). An additional negative damping is in general desirable, but a positive damping, which may destabilize the torsional modes, is also possible. Figure 8 indeed shows that the first weakly coupled torsional eigenvalue ($f_1 = 812$ rpm) becomes slightly unstable at 1740 rpm. Obviously the instability whirl tends to lock in at the lowest system frequency, which in the coupled case may be a bending or a torsional mode. Because negative torsional damping is always present in real machines (material damping, damping of the surrounding media), the slight torsional instability of our coupled model would not occur in practice. The next eigenvalue, which becomes clearly unstable at 3510 rpm, belongs to the second strongly torsional-lateral-coupled mode ($f_2 = 1871$ rpm). Its threshold speed is 7 percent lower than in the uncoupled case. In addition, the third eigenvalue, which remains stable in the uncoupled case, becomes unstable at a rotational speed of 4150 rpm in the torsional-lateral-coupled model. The corresponding eigenfrequency and eigenvector (an almost pure bending mode lying in the x-y plane, which is perpendicular to the plane of tooth force action) nearly coincide with the solutions of the uncoupled system (fig. 7). Therefore we conclude that although we cannot recognize a strong torsional-lateral coupling in the frequencies and modes, the coupling may still affect the stability behavior. This effect is due to the energy exchange between the torsional and bending vibrations at the gear mesh (fig. 6).

It is important to note that the instability onset speed of the uncoupled and the torsional-lateral-coupled systems are not equal. The coupling mechanism in gears may essentially lower the threshold speed. Classical uncoupled stability analysis indicates that the system becomes unstable at the lowest lateral threshold speed of the individual rotors. In a coupled analysis the actual stability threshold may occur in a torsional or a strongly torsional-lateral-coupled mode of the complete system.

DISCUSSION OF STABILITY BEHAVIOR

In a classical vibration analysis, which ignores the coupling between torsional and lateral vibrations in gears, the torsional critical speeds are only sensitive to torsional system parameters whereas the lateral eigenvalues of an individual rotor depend only on its bending parameters. We use the expression "torsional parameter" in this context for rotary inertia or torsional stiffness and "bending parameters" for quantities such as mass or flexural stiffness. If we consider torsional and bending vibrations as coupled in the gear, an eigenvalue is generally sensitive to torsional and bending parameters of all shafts. The effect of the coupling on the stability behavior of the complete rotor system can therefore be studied by answering the questions

- (1) How do modifications of torsional and bending system parameters change the stability threshold? (Parameter study)
- (2) How do changes of torsional and bending system parameters affect the damping constant of the eigenvalues? (Sensitivity analysis)

Parameter Studies

For the parameter study two torsional parameters and two bending parameters of the simple shaft system were selected (fig. 10). Figures 11 and 12 show how the stability threshold speed due to the zero passage of the second eigenvalue (real part) changes when the chosen system parameters are varied. As a reference model we take the torsional-lateral-coupled model with the data of figure 3. Its second eigenvalue becomes unstable at a speed of 3510 rpm. The question is now: How do respective torsional bending parameters affect this instability onset speed?

Figure 11 shows the influence of the torsional stiffness \widehat{k}_2 and rotary inertia θ_2 of shaft 2. Of course the torsional parameters do not change the stability threshold in the uncoupled model. In the coupled case, the rise of the torsional stiffness \widehat{k}_2 stabilizes the second eigenvalue, but a higher rotary inertia θ_2 destabilizes it. At first sight (fig. 11) it appears that a torsionally stiffer shaft 2 would make the system more stable. But when the second eigenvalue becomes more stable, the first eigenvalue is destabilized; therefore the stability threshold of the coupled system is lowered by an increased torsional stiffness. Decreasing the rotary inertia θ_2 produces similar results. This effect is ignored in figure 11 because only the real part of the second eigenvalue is considered.

Figure 12 shows that the influence of the bending parameters on the threshold speed for the second eigenvalue is much stronger than the influence of the torsional parameters. It is again interesting to note that the instability onset speed essentially depends on whether an uncoupled or a torsional-lateral-coupled model is used. In our case a stiffer shaft 1 (k_1) with a smaller mass m_1 makes the system more stable. In both cases the stability threshold for the coupled model is lower than for the uncoupled one.

We conclude from this study that the stability threshold speed is substantially influenced (1) by the model used in the coupled or uncoupled case and (2) by the torsional and bending system parameters in the coupled case. This fact indicates a strong torsional-lateral coupling relation to the stability behavior.

Sensitivity Analysis

As a second tool to investigate the influence of the torsional-lateral coupling, we used a sensitivity analysis of the eigenvalues. This method yields so-called influence coefficients, which describe the change of an eigenvalue λ_n caused by a small modification of a system parameter p_k . The influence coefficients for the real parts of the eigenvalues express how sensitive the stability of the system is to parameter changes. The stability threshold of an uncoupled model is only affected by the bending parameters of the individual rotors. In contrast to that for the torsional-lateral-coupled system, an eigenvalue is generally influenced by torsional and bending parameters of all shafts. Therefore by the aid of the sensitivities of the real eigenvalue parts for the uncoupled and coupled systems, the influence of the torsional-lateral coupling on the stability behavior can be discussed.

This sensitivity analysis is based on an expansion of the eigenvalues in terms of the generalized system parameters p_k , where the p_k may be mass, damping, stiffness, or even physical parameters, for example, bearing clearance (ref. 8):

$$\lambda_n = \lambda_{n,0} + \frac{\partial \lambda_n}{\partial p_{1/0}} \cdot \Delta p_1 + \frac{\partial \lambda_n}{\partial p_{2/0}} \cdot \Delta p_2 + \dots + \frac{\partial \lambda_n}{\partial p_{k/0}} \cdot \Delta p_k \quad (11)$$

Truncation of Taylor's expansion after the first derivatives leads to a linear approximate formula. It is shown in references 8 to 10 that the eigenvalue derivatives can be expressed by the eigenvalues, by the left- and right-hand eigenvectors of the original system (subscript 0), and by derivatives of the system matrices \tilde{M} , \tilde{D} , and \tilde{K} to the parameters p_k (subscript k).

$$\frac{\partial \lambda_n}{\partial p_{k/0}} = - \frac{1}{\lambda_n} (\lambda_n^2 \cdot \tilde{M}_{,k} + \lambda_n \tilde{D}_{,k} + \tilde{K}_{,k}) r_{n/0} = g_{n,k} \quad (12)$$

The eigenvectors must be normalized in a special way (ref. 10). The derivatives are also called influence coefficients.

For the simple gear model we start from a point near the stability threshold speed and investigate how particular parameters affect the stability behavior. Figure 13 shows the influence of the torsional stiffness \hat{k}_2 on the real and the imaginary part of the second eigenvalue. It can be seen that increasing the torsional stiffness has a stabilizing effect on the second eigenvalue. The corresponding influence coefficient calculated with the given linear formula is indicated by the tangent to the curve.

Figure 14 contains influence coefficients for the elements used in our gear model such as disks, journal bearings, and beams. The influence coefficients in equation (12) represent an absolute measure for the changes of the complex eigenvalues $\lambda_n = \alpha_n + i\omega_n$ caused by parameter modifications. By means of these coefficients a relative measure, the nondimensional sensitivity, can be defined:

$$\frac{\Delta \alpha_n / |\alpha_n|}{\Delta p_k / p_k} = S_{n,k}^\alpha = \operatorname{Re}(g_{n,k}) \cdot \frac{p_k}{\alpha_n} \quad (13)$$

$$\frac{\Delta \omega_n / \omega_n}{\Delta p_k / p_k} = S_{n,k}^\omega = \operatorname{Im}(g_{n,k}) \cdot \frac{p_k}{\omega_n}$$

where $S_{n,k}^\alpha$ is the nondimensional sensitivity of the damping coefficient and $S_{n,k}^\omega$, of the natural frequency. This presentation has the great advantage that the influence of several parameters on different modes can be compared immediately.

To show the influence of torsional and bending system parameters on the stability behavior of our rotor system, relative sensitivities for the real part of the second eigenvalue were calculated near the threshold speed of the uncoupled and coupled models ($n_1 = 3680$ rpm) and are plotted in figure 15. It is important to note that the values of the relative sensitivities for the uncoupled and coupled models are different.

Of course in the uncoupled model the torsional parameters do not affect the real part of the second eigenvalue, which belongs to a pure bending mode. The corresponding sensitivities are therefore equal to zero.

Nevertheless in the uncoupled model changes of the bending parameters of shaft 1 have a strong influence on the real part of the second eigenvalue. Because the oil-film bearings are relatively stiff as compared with the bending stiffness of shaft 1, the changes of the shaft parameters (e.g., bending stiffness, mass of the pinion) have a much stronger effect on the damping constant than do the bearing parameters (e.g., clearance Ψ). In the uncoupled case the bending of the rigidly supported shaft 2 is not related to the oil-film-supported shaft 1, which becomes unstable. Therefore the bending parameters of shaft 2 have no influence on the stability behavior.

In the coupled model it is obvious that changes of the torsional parameters can have a strong influence on the real part of the second eigenvalue. A comparison of the different torsional parameters points out that the main influence is from the torsional parameters of shaft 2. Their relative sensitivities are much greater than those of the torsional parameters of shaft 1. A look at the torsional components of the corresponding second mode makes the reasons clear: shaft 2 shows a maximum displacement because of torsion at the gear wheel and is much more twisted than shaft 1.

The sensitivity of the torsional stiffness has a negative sign. An increasing stiffness stabilizes the rotor system, as we have already seen in the parameter study (figs. 11 and 13). The rotatory inertia of the second gear wheel and of the generator have a positive sensitivity. Increasing values of this parameter have a destabilizing effect (fig. 11).

Changes of the bending parameters have a stronger effect on the real part of the second eigenvalue than do the torsional parameters. Because the bending of shaft 2 is for the coupled model connected to the oil-film-supported shaft 1 by the coupling equation (2), its parameters also influence the stability behavior of our model. But as shaft 2 is almost too rigid to bend in the second mode the influence coefficients of its parameters (e.g., mass of the wheel and lateral stiffness) are relatively small.

Obviously the dimensionless sensitivities of the bending parameters of shaft 1 differ essentially from the values of the uncoupled model. For example, the influence coefficient of the clearance for the right bearing in the coupled case is of about the same magnitude as that in the uncoupled case but has the opposite sign. The sensitivities of the bending stiffness and the mass of the pinion are essentially smaller than those in the uncoupled model.

The results show that the stability behavior of our model is particularly influenced by the bending parameters of shaft 1 and the torsional parameters of shaft 2. The differences in the solutions for the sensitivities in the

uncoupled and coupled models indicate that the torsional-lateral coupling must not be neglected in discussing the stability behavior of geared rotors.

CONCLUSIONS

In this paper a study of the stability behavior is given for a simple geared shaft system. It is shown that the classical eigenvalue analysis, which ignores the coupling of torsional and lateral vibrations in gears, may lead to serious errors in the prediction of the stability onset speed, the critical speeds, and the natural modes. Also it does not account for the damping of the torsional modes, which is attributed to the lateral motions in the journals.

The strong relation of torsional-lateral coupling to stability behavior is proven by parameter studies and sensitivity analysis, which show the influence of torsional and bending system parameters on the stability threshold and damping constants.

The analytical results for the simple geared model remain to be verified by experimental investigations and extended to more complex rotor systems.

REFERENCES

1. Wachel, J.C.; and Szenasi, F.R.: Field Verification of Lateral-Torsional Coupling Effects on Rotor Instabilities in Centrifugal Compressors. NASA CP-2147, 1980.
2. Yamada, T.; and Mitsui, J.: A Study on the Unstable Vibration Phenomena of a Reduction Gear system, Including the Lightly Loaded Journal Bearings for a Marine Steam Turbine. Bull. JSME, Vol. 22, No. 163, 1979.
3. Iannuzzelli, R.J.; and Elward, R.M.: Torsional-Lateral Coupling in Geared Rotors. ASME No. 84-GT-71, 1984.
4. Simmons, H.R.; and Smalley, A.J.: Lateral Gear Shaft Dynamics Control Torsional Stresses in Turbine Driven Compressor Train. ASME No. 84-GT-28, 1984.
5. Dubois, G.B.; and Ocvirk, F.W.: Analytical Derivation and Experimental Evaluation of Short-Bearing Approximation for Full Journal Bearings. NACA Report 1157, 1953.
6. Ott, H.H.: Zylindrisches Gleitlager bei instationärer Belastung. Dissertation ETH Zurich, 1948.
7. Lund, J.W.: Critical Speeds, Stability and Response of a Geared Train of Rotors. ASME No. 77-DET-30, 1977.
8. Iida, H.; Tamura, A.; Kikuch, K; and Agata, H.: Coupled Torsional-Flexural Vibration of a Shaft in a Geared System of Rotors. Bull. JSME, Vol. 23, No. 1986, Dec. 1980.

9. Glienicke, J.: Feder- und Dämpfungskonstanten von Gleitlagern und deren Einfluss auf das Schwingungsverhalten eines einfachen Rotors. (Stiffness and Damping Coefficients in Journal Bearings). Thesis TH Karlsruhe, 1966.
10. Fritzen, C.P.; and Nordmann, R.: Influence of Parameter Changes to the Stability Behavior of Rotors. Rotordynamic Instability Problems in High-Performance Turbomachinery. NASA CP-2250, 1982.

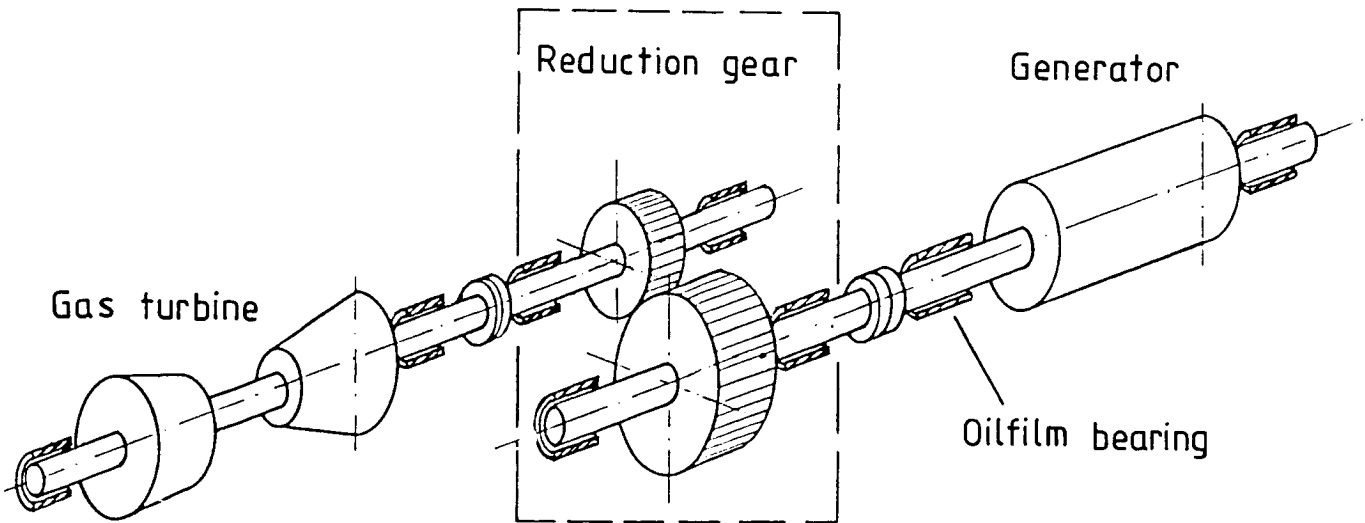


Figure 1. - Reduction gear in a turbogenerator set.

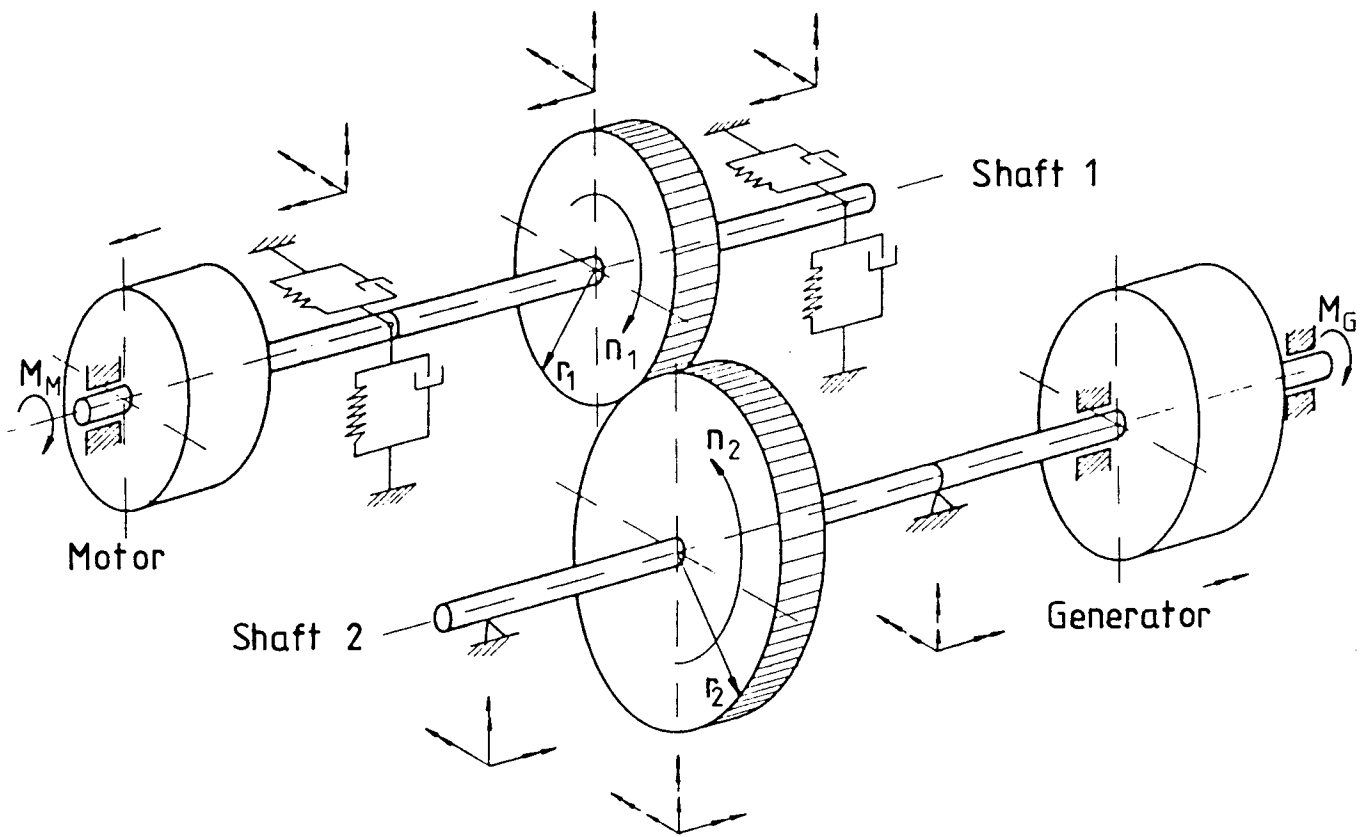


Figure 2. - Model of a geared rotor system.

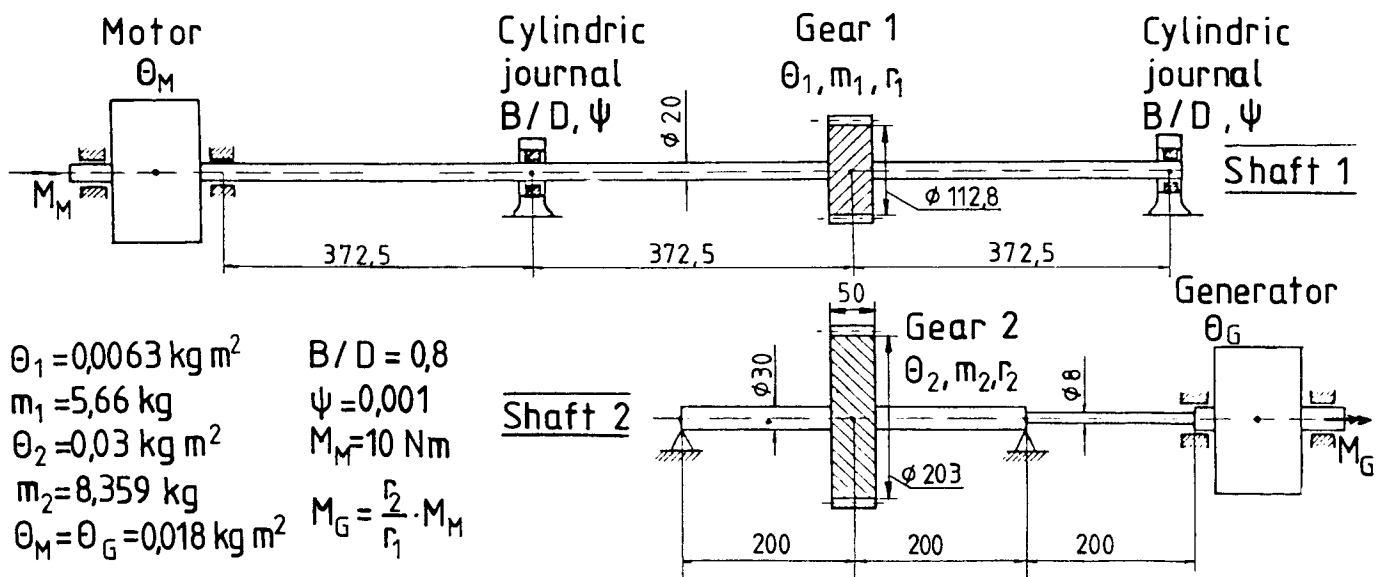
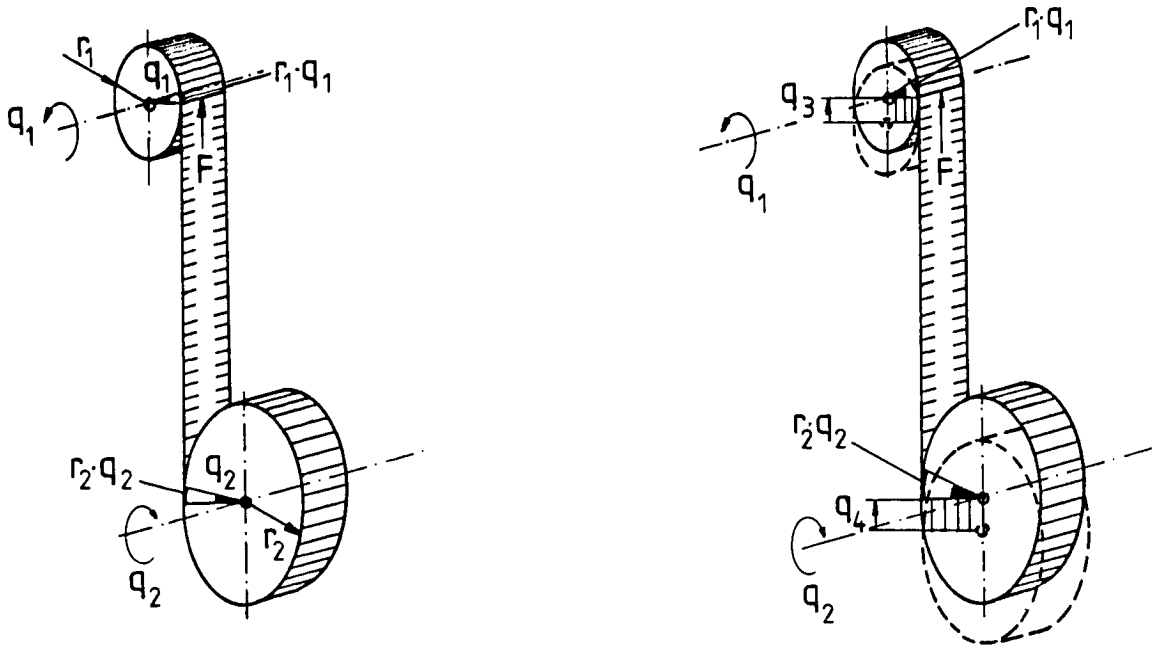


Figure 3. - Data for the geared rotor system.



Kinematic constraint without lateral displacement of gear wheels

$$r_1 q_1 = r_2 q_2$$

Kinematic constraint with lateral displacement of gear wheels

$$r_1 q_1 + q_3 = r_2 q_2 + q_4$$

Figure 4. - Kinematic constraints in a gear stage.

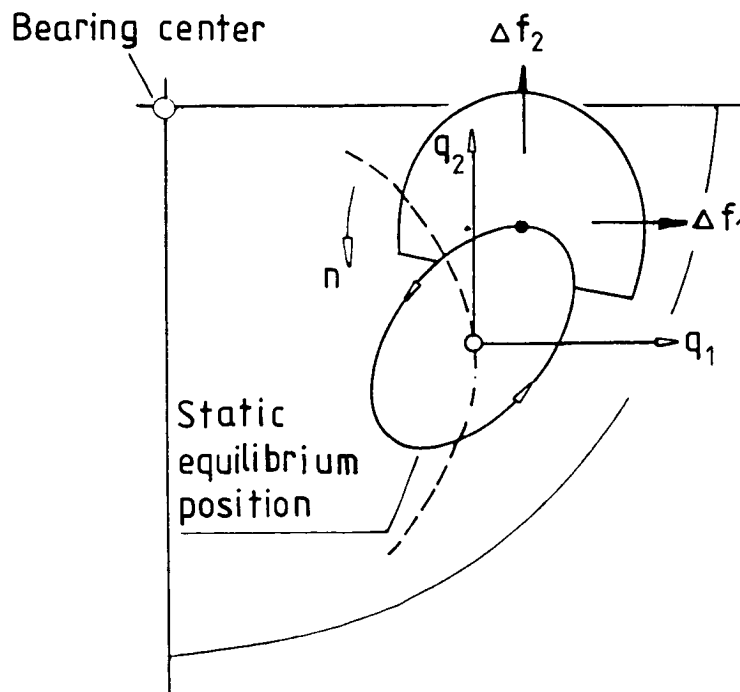
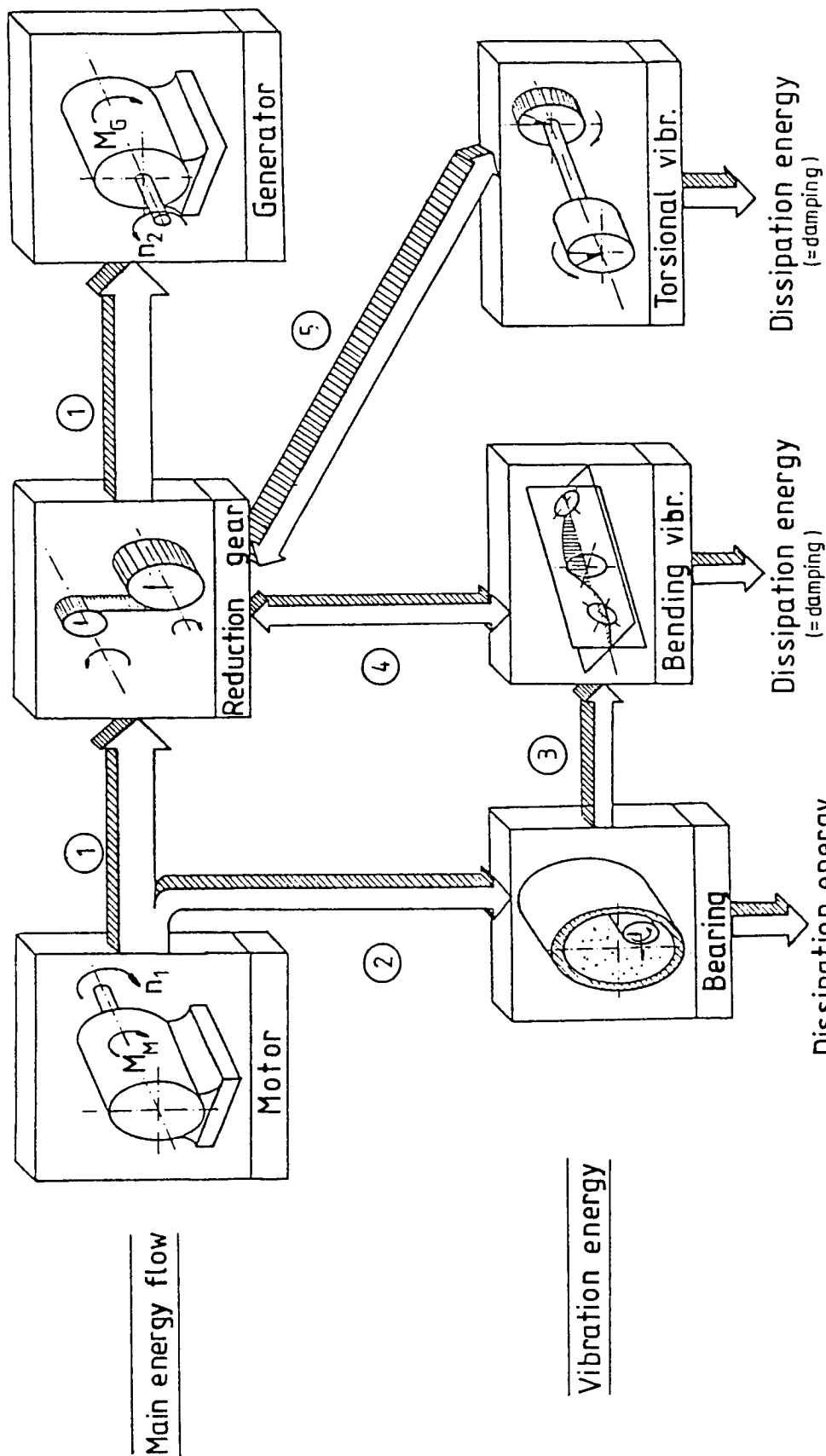


Figure 5. - Vibrations of the journal.



- ① Main energy flow from motor to generator.
- ② Energy flow branching off the main flow due to shear forces in the oilfilm.
- ③ Energy flowing from the oilfilm to the shaft bending vibrations.
- ④ Energy flowing from bending vibrations in the gear mechanism and back.
- ⑤ Energy flowing from the lateral excited gear wheels to the torsional motion and back, due to torsional-lateral coupling.

Figure 6. - Energy flow in a geared system with oilfilm excited torsional-lateral vibrations (schematic).

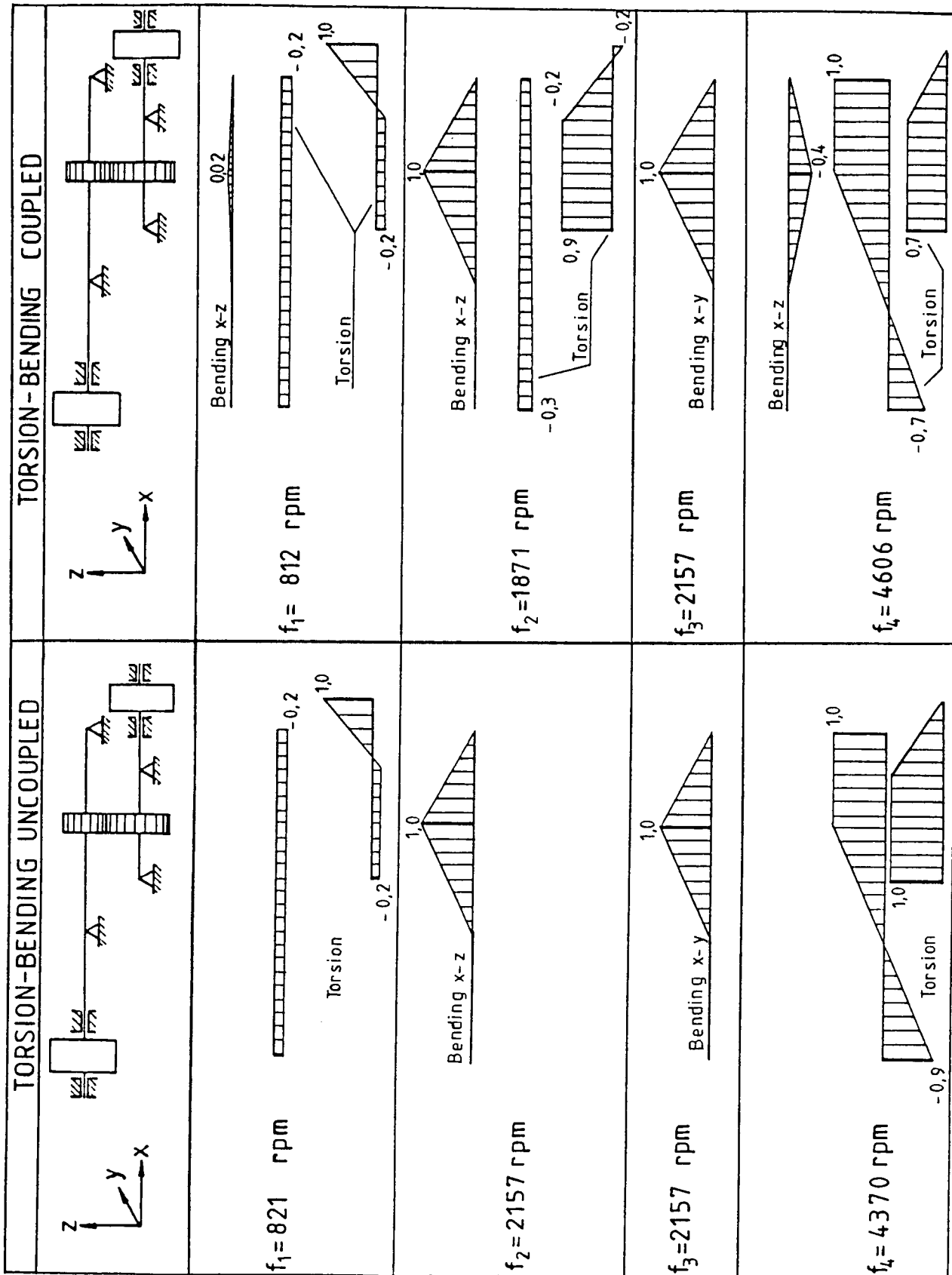
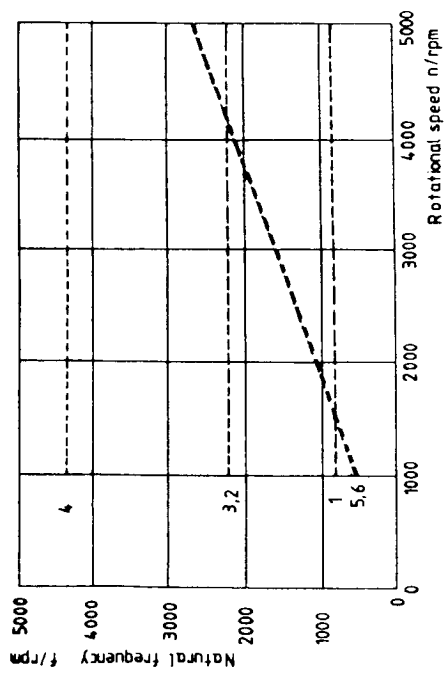


Figure 7. - Eigenfrequencies and eigenvectors of the rigidly supported gear system (ref. 9).

TORSION - BENDING UNCOUPLED



TORSION - BENDING COUPLED

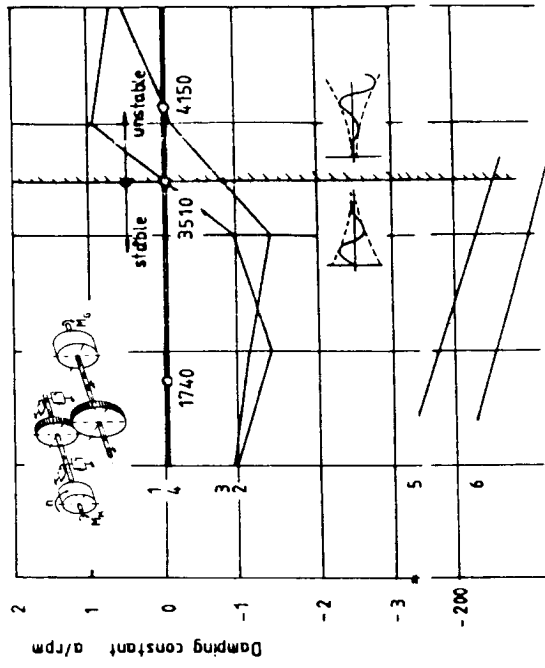
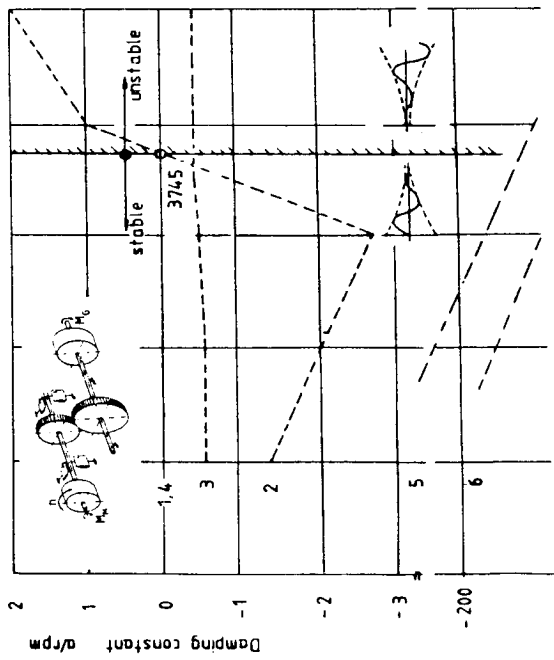
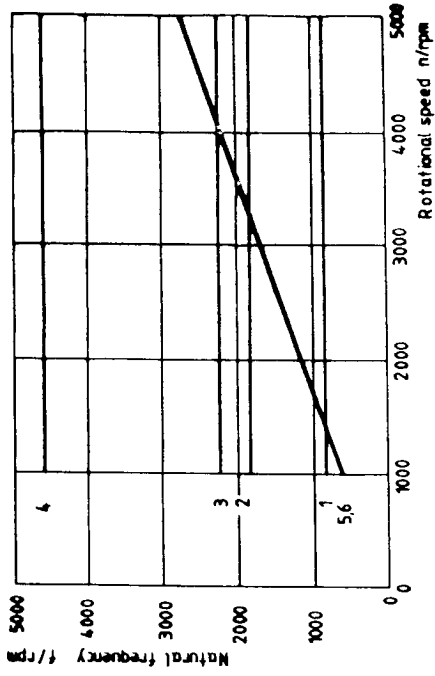


Figure 8. - Eigenfrequencies and damping for the uncoupled and torsional-lateral coupled system.

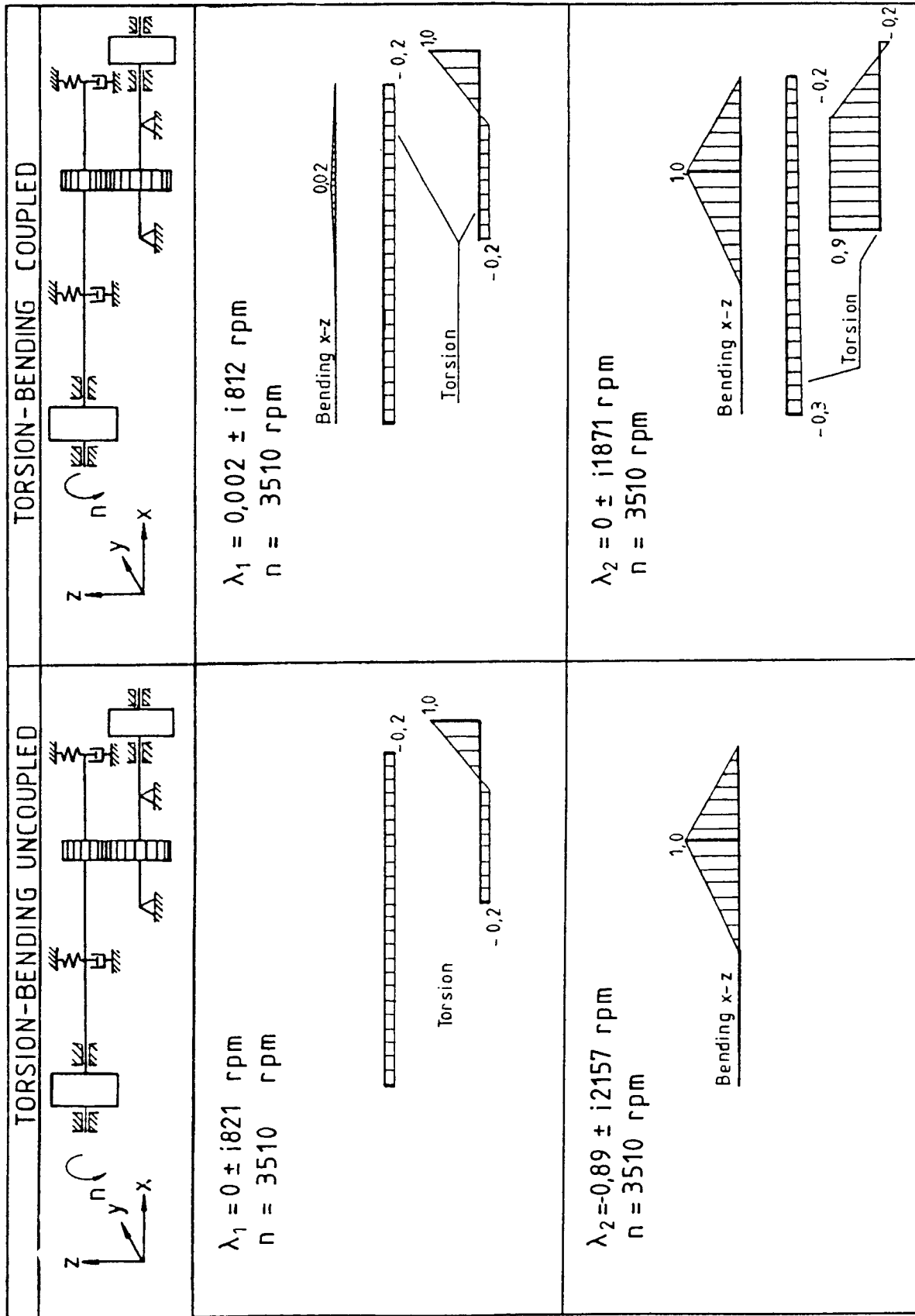
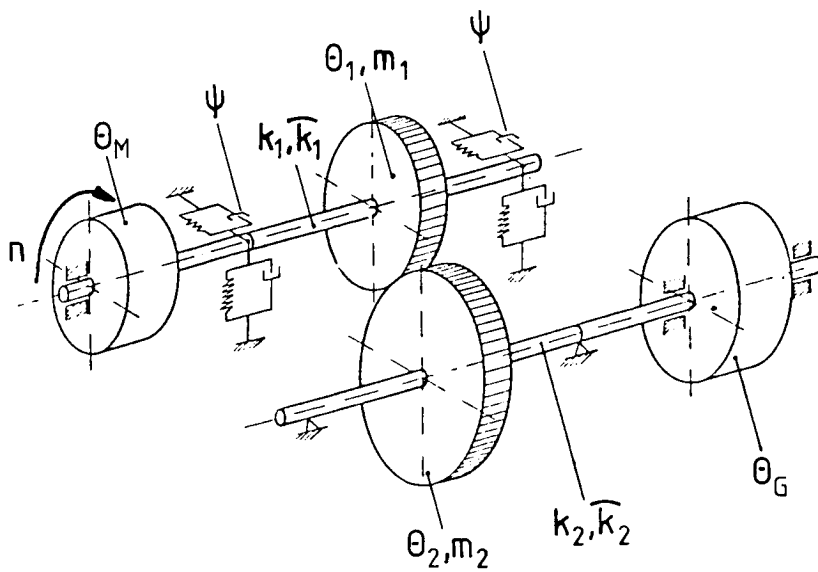


Figure 9. - First and second eigenvector of the uncoupled and torsional-lateral coupled system at the stability threshold (in the moment of maximum lateral displacement).



	Bending	Torsion
m_1	●	
m_2	○	
θ_M		○
θ_1		○
θ_2		●
θ_G		○
ψ	○	
k_1	●	
k_2	○	
\bar{k}_1		○
\bar{k}_2		●

● Varied parameters

Figure 10. - Variation of parameters.

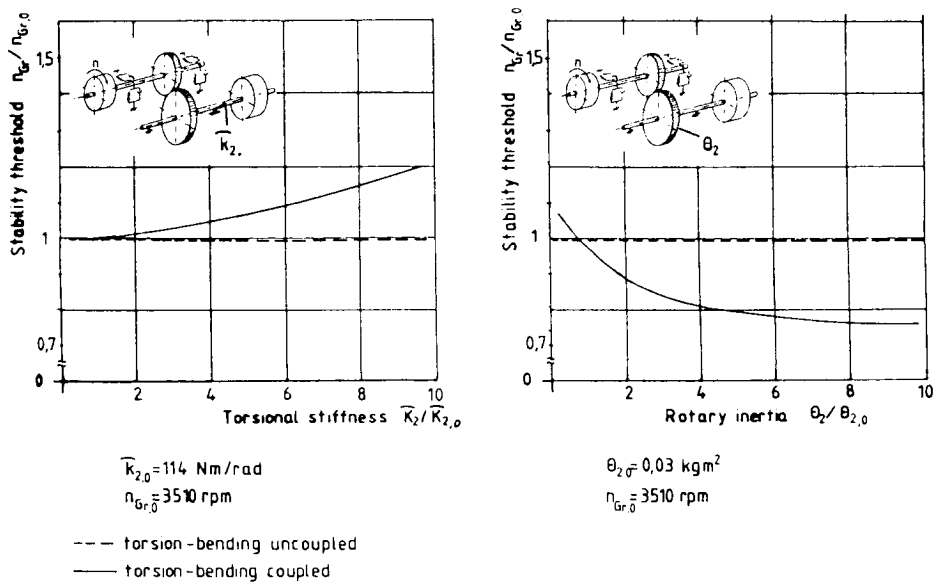


Figure 11. - Influence of torsional parameters on the stability threshold.

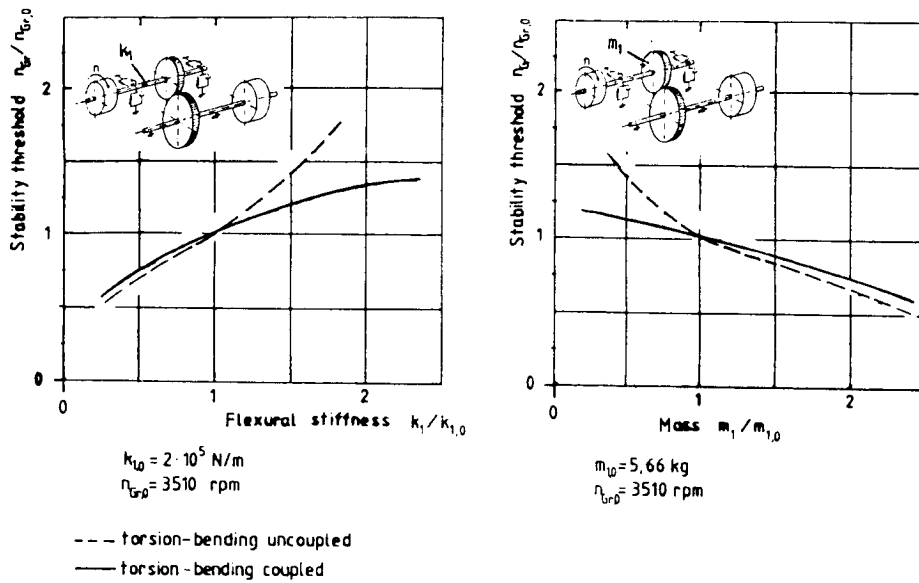


Figure 12. - Influence of bending parameters on the stability threshold.

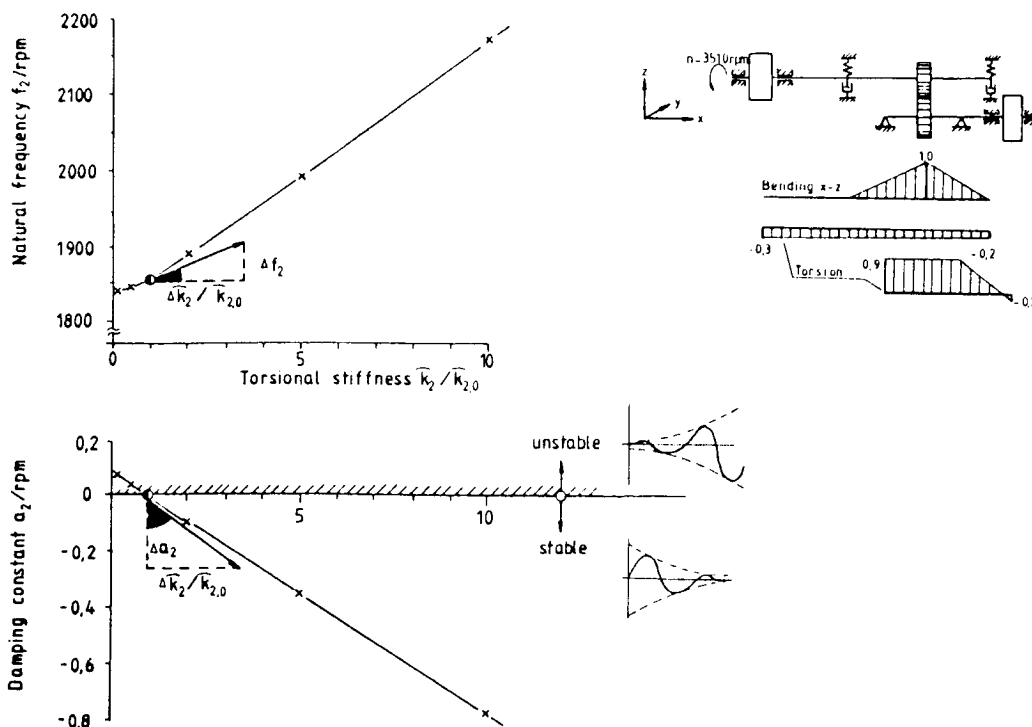


Figure 13. - Effect of change in torsional stiffness \hat{k}_2 to the second eigenvalue for the torsional-lateral coupled system.

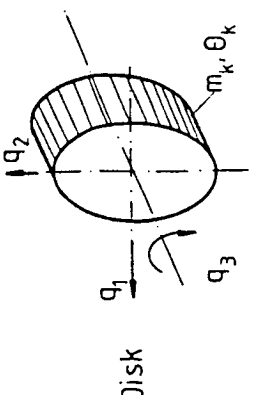
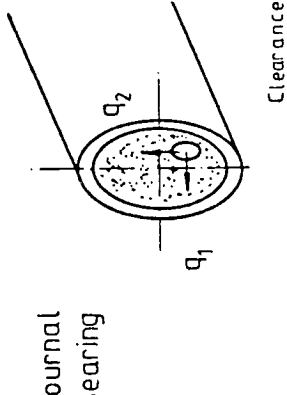
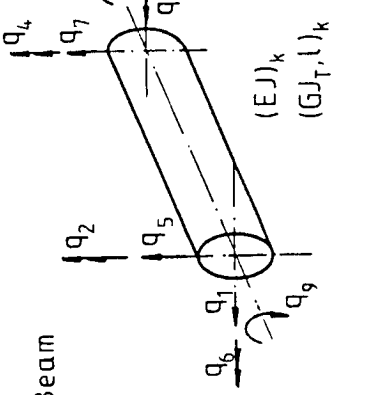
Element	Force - Motion - Relation	Influence-Coefficient g_{nk}
 <p>Disk</p>	<p>Bending: $\begin{bmatrix} F_1 \\ F_2 \end{bmatrix} = \begin{bmatrix} m_k & 0 \\ 0 & m_k \end{bmatrix} \begin{bmatrix} q_1 \\ q_2 \end{bmatrix}$</p> <p>Torsion: $F_3 = \theta_k \cdot \dot{q}_3$</p>	<p>Bending: $g_{nk} = \frac{\partial \lambda_n}{\partial m_k} = -\lambda_n^2 (l_1 r_1 + l_2 r_2)_n$</p> <p>Torsion: $g_{nk} = \frac{\partial \lambda_n}{\partial \theta_k} = -\lambda_n^2 (l_3 r_3)_n$</p>
 <p>Journal Bearing</p>	$\begin{bmatrix} F_1 \\ F_2 \end{bmatrix} = \begin{bmatrix} c_{11} & c_{12} \\ c_{21} & c_{22} \end{bmatrix} \begin{bmatrix} \dot{q}_1 \\ \dot{q}_2 \end{bmatrix} + \begin{bmatrix} k_{11} & k_{12} \\ k_{21} & k_{22} \end{bmatrix} \begin{bmatrix} q_1 \\ q_2 \end{bmatrix}$	<p>Bending: $g_{nk} = \frac{\partial \lambda_n}{\partial \psi_k} = \sum_{i=1}^2 \sum_{j=1}^2 \frac{\partial \lambda_n}{\partial c_{ij}} \cdot \frac{\partial c_{ij}}{\partial \psi_k} + \frac{\partial \lambda_n}{\partial k_{ij}} \cdot \frac{\partial k_{ij}}{\partial \psi_k}$</p> $= \sum_{i=1}^2 \sum_{j=1}^2 -\lambda_n (l_i r_j)_n \frac{\partial c_{ij}}{\partial \psi_k} - (l_i r_j)_n \frac{\partial k_{ij}}{\partial \psi_k}$
 <p>Beam</p>	<p>Bending: $\begin{bmatrix} F_1 \\ \vdots \\ F_8 \end{bmatrix} = EJ \begin{bmatrix} K_{11} & \dots & K_{18} \\ \vdots & \ddots & \vdots \\ K_{81} & \dots & K_{88} \end{bmatrix}_k \begin{bmatrix} q_1 \\ \vdots \\ q_8 \end{bmatrix}$</p> <p>Torsion: $\begin{bmatrix} F_9 \\ F_{10} \end{bmatrix} = \frac{GJ_T}{l} \begin{bmatrix} 1 & -1 \\ -1 & 1 \end{bmatrix}_k \begin{bmatrix} q_9 \\ q_{10} \end{bmatrix}$</p>	<p>Bending: $g_{nk} = \frac{\partial \lambda_n}{\partial (EJ)_k} = -[l_1 \dots l_8]_n \begin{bmatrix} K_{11} & \dots & K_{18} \\ \vdots & \ddots & \vdots \\ K_{81} & \dots & K_{88} \end{bmatrix}_k \begin{bmatrix} r_1 \\ \vdots \\ r_8 \end{bmatrix}_n$</p> <p>Torsion: $g_{nk} = \frac{\partial \lambda_n}{\partial (GJ_T)_k} = -[l_9, l_{10}]_n \begin{bmatrix} 1 & -1 \\ -1 & 1 \end{bmatrix}_k \begin{bmatrix} r_9 \\ r_{10} \end{bmatrix}_n$</p>

Figure 14. - Influence coefficients for the disk, journal bearing, and beam elements.

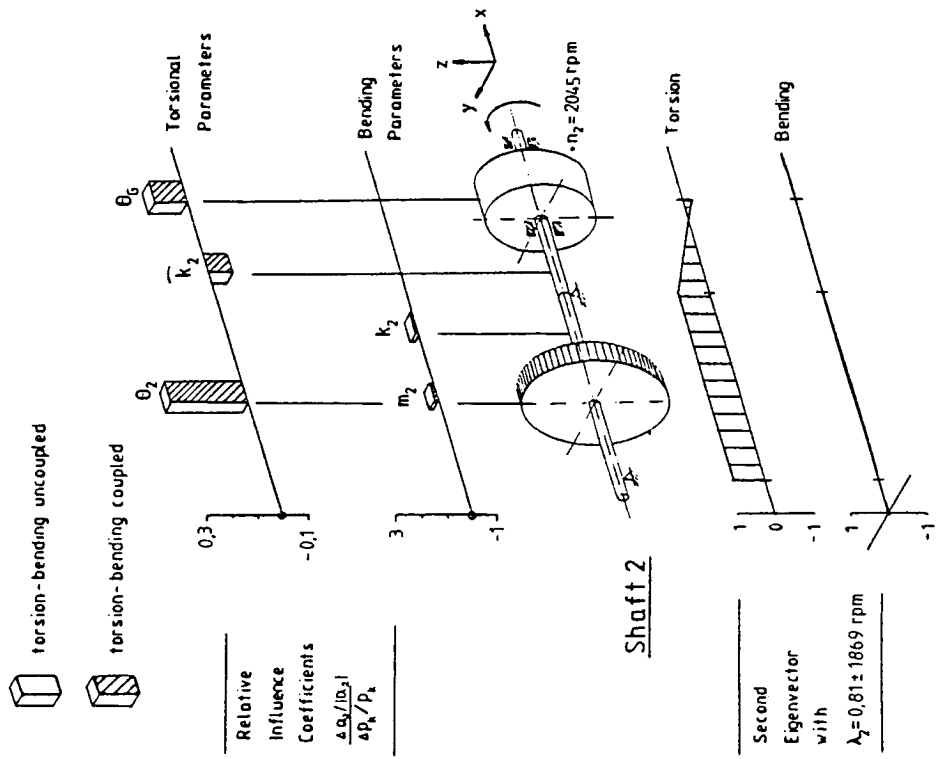


Figure 15. - Sensitivities of the second eigenvalue.